



HHS Public Access

Author manuscript

Cell Chem Biol. Author manuscript; available in PMC 2017 April 21.

Published in final edited form as:

Cell Chem Biol. 2016 April 21; 23(4): 443–452. doi:10.1016/j.chembiol.2016.03.010.

GNF-2 inhibits dengue virus by targeting Abl kinases and the viral E protein

Margaret J. Clark^{a,*}, Chandra Miduturu^{b,c,*}, Aaron G. Schmidt^d, Xuling Zhu^a, Jared D. Pitts^a, Jinhua Wang^{b,c}, Supanee Potisopon^a, Jianming Zhang^{b,c}, Amy Wojciechowski^{b,c}, Justin Jang Hann Chu^a, Nathanael S. Gray^{b,c}, and Priscilla L. Yang^{a,#}

^aDepartment of Microbiology and Immunobiology, Harvard Medical School 77 Avenue Louis Pasteur, Boston, MA 02115, USA

^bDepartment of Cancer Biology, Dana-Farber Cancer Institute, Boston, MA 02115, USA

^cDepartment of Biological Chemistry & Molecular Pharmacology, Harvard Medical School, 360 Longwood Ave, Longwood Center LC-2209, Boston, MA 02115, USA

^dLaboratory of Molecular Medicine, Children's Hospital, Harvard Medical School, Boston MA 02115, USA

Summary

Dengue virus infects over 300 million people annually, yet there is no widely protective vaccine or drugs against the virus. Efforts to develop antivirals against classical targets such as the viral protease and polymerase have not yielded drugs that have advanced to the clinic. Here we show that the allosteric Abl kinase inhibitor GNF-2 interferes with dengue virus replication via activity mediated by cellular Abl kinases but additionally blocks viral entry via an Abl-independent mechanism. To characterize this newly discovered antiviral activity, we developed disubstituted pyrimidines that block dengue virus entry with structure-activity relationships distinct from those driving kinase inhibition. We demonstrate that biotin- and fluorophore-conjugated derivatives of GNF-2 interact with the dengue glycoprotein, E, in the prefusion conformation that exists on the virion surface and that this interaction inhibits viral entry. This study establishes GNF-2 as an antiviral compound with polypharmacological activity and provides 'lead' compounds for further optimization efforts.

Graphical abstract

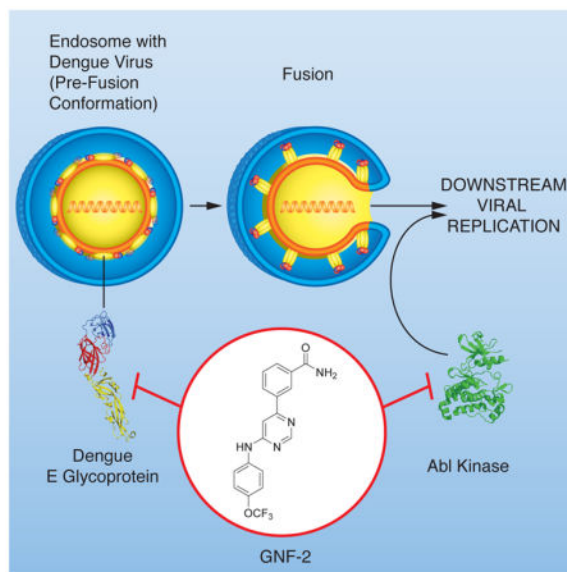
[#]To whom correspondence should be addressed: Priscilla L Yang, 77 Avenue Louis Pasteur, Boston, MA 02115, 617-432-5415, priscilla_yang@hms.harvard.edu.

^{*}Contributed equally

Author Contributions

C.M., M.J.C., A.S., X.Z., J.D.P., J.W., S.P., J.Z., A.W., and J.J.H.C. performed experiments and interpreted data. C.M., A.S., M.J.C., J.D.P., X.Z., P.L.Y., and N.S.G. designed experiments and interpreted data. P.L.Y. and N.S.G. secured funding. P.L.Y. wrote the manuscript with feedback from all co-authors. J.D.P. and J.W. assisted with preparation of figures and tables.

Publisher's Disclaimer: This is a PDF file of an unedited manuscript that has been accepted for publication. As a service to our customers we are providing this early version of the manuscript. The manuscript will undergo copyediting, typesetting, and review of the resulting proof before it is published in its final citable form. Please note that during the production process errors may be discovered which could affect the content, and all legal disclaimers that apply to the journal pertain.



INTRODUCTION

Dengue virus (DENV) is a mosquito-borne virus and member of the *Flavivirus* genus of enveloped, positive-stranded RNA viruses that include West Nile virus (WNV), Japanese encephalitis virus (JEV), and other human and animal pathogens. Comprised by four related serotypes of virus (DENV1-4), DENV is currently estimated to infect over 300 million humans annually (Bhatt, et al., 2013). DENV infection causes a broad spectrum of disease ranging from classical dengue fever to dengue hemorrhagic fever and dengue shock syndrome characterized by plasma leakage that is potentially fatal. There is currently no broadly protective or widely available vaccine nor are there specific antiviral therapies. Due to the challenges encountered in developing a safe vaccine that confers durable protection against all four DENV serotypes, there is considerable interest in antivirals that can reduce transmission and ameliorate disease.

Most clinically used antiviral drugs against human immunodeficiency virus (HIV) or hepatitis C virus (HCV) target essential virally encoded enzymes such as polymerases or proteases. Inhibitors of these enzymes are typically identified by target-based screening and optimized via structure-based drug design. To complement this traditional approach, we have used cellular phenotypic screens performed with infectious dengue virus to identify in an unbiased fashion compounds that could interfere with any process in the viral replication cycle (Carocci, et al., 2015; Chu and Yang, 2007). Although we have focused primarily on small collections of well-curated compounds with known targets, the screens could identify compounds that act via both host and viral targets. Here we show that GNF-2, a well-established allosteric inhibitor of Abl kinases, has antiviral activity that derives from both its known kinase target as well as additional antiviral activity due to interactions with the E protein on the virion surface.

RESULTS

Abl kinase inhibitors have anti-dengue viral activity

In search of inhibitors of DENV replication, we previously performed a cellular phenotypic screen for known kinase inhibitors that prevented infection and replication of DENV (Chu and Yang, 2007). This effort identified several clinically approved inhibitors of BCR-Abl kinase including imatinib and dasatinib, which are ATP-competitive inhibitors of Abl kinase activity. Although dasatinib's anti-DENV activity was primarily attributed to inhibition of DENV genome replication mediated by Fyn kinase, cellular Abl kinase (c-Abl) was also suspected to mediate antiviral activity based on significant inhibition of DENV by other, unrelated inhibitors of Abl kinases that lack activity against Fyn and other Src family kinases (Chu and Yang, 2007; de Wispelaere, et al., 2013). Imatinib and GNF-2 (Figure 1A) inhibit Abl kinases with comparable potency in biochemical and cell-based assays (Adrian, et al., 2006) but do so via different mechanisms. Whereas imatinib binds in the kinase ATP-binding site, GNF-2 inhibits kinase activity allosterically through binding in a myristate-binding pocket unique to Abl kinases. In initial dose-response studies quantifying the antiviral activity of imatinib and GNF-2 against the New Guinea C (NGC) strain of dengue virus serotype 2 (DENV2 NGC), GNF-2 exhibits more antiviral activity than imatinib in single-cycle virus yield reduction assays (Figure 1B). To determine at what point in the viral replication cycle that imatinib and GNF-2 exert their antiviral effect(s) we performed time-of-addition experiments and measured the viral yield produced from a single-cycle of infection via viral plaque assay. Specifically, the inhibitors were individually 1) pre-incubated with viral inoculum or with cells, 2) present during a one-hour infection period, or 3) added at different time points post-infection (Figure 1C). Imatinib exhibits no effect on DENV2 when pre-incubated with cells or viral inoculum or when present during the initial infection but has considerable antiviral activity when added as late as five hours post-infection. This antiviral activity appears to be shared with GNF-2; however, GNF-2 exhibits additional antiviral activity when pre-incubated with the viral inoculum prior to infection (Figure 1C). We reasoned that the anti-DENV2 activity observed in the post-infection window is mediated by a cellular Abl kinase since imatinib and GNF-2 share no other known molecular targets. This interpretation is supported by the observation that DENV2 replication is significantly decreased when c-Abl is targeted by RNAi (Figure 1D) as well as in a murine embryo fibroblast cell line genetically deficient for c-Abl (Koleske, et al., 1998) when compared to wild-type 3T3 cells (Figure 1E). Collectively these genetic and pharmacological studies suggest that the kinase activity of c-Abl is important for efficient DENV2 replication and that the inhibition of DENV2 by imatinib and GNF-2 post-infection is mediated by c-Abl kinase.

GNF-2 inhibits DENV2 via an Abl-independent mechanism

Because the time-of-addition experiments indicated that GNF-2 has an anti-DENV2 activity lacked by imatinib, we characterized this activity further to identify potential molecular target(s). To test the hypothesis that this activity is independent of Abl kinases, we prepared a number of GNF-2 analogs designed to engineer out the Abl-inhibitory activity and to provide probes to identify additional cellular or viral targets accounting for GNF-2's potency as an antiviral. Since the anti-DENV activity mediated by Abl kinases appears to occur

relatively late in the DENV replication cycle, we used a viral infectivity assay that minimized potential contributions of Abl kinases to antiviral activity by limiting compound treatment to a pre-incubation with the viral inoculum, conducting the initial infection at a multiplicity of infection (MOI) of 1 (Figure 2A). The inhibitors were removed by washing the infected cell monolayers, and fresh medium lacking inhibitor was overlaid for the remaining 23 hours of the single-cycle viral infection. The viral yield was then quantified as a measure of the efficiency of the infection performed twenty-four hours prior. To assess the inhibitory activity of compounds against Abl kinases, we used BCR-Abl transformed Ba/F3 cells, which are dependent on BCR-Abl activity for proliferation and viability and provide a sensitive assay for detecting inhibition of intracellular Abl kinase activity (Adrian, et al., 2006).

To explore the structure-activity relationships (SAR) for the Abl kinase-dependent and Abl kinase-independent anti-DENV activities of GNF-2, we took advantage of our prior work exploring the structural requirements for maintaining potent Abl inhibitory activity and introduced modifications that were likely to block binding to the myristate pocket of Abl (Deng, et al., 2010). We synthesized a series of analogs based upon the 4, 6-disubstituted core structure of GNF-2 with either the 4-trifluoromethoxy aniline or the aryl benzamido portions held constant. In addition, since both 2,4- and 4,6-disubstituted pyrimidines are privileged structures widely incorporated in kinase inhibitors, regioisomeric 2,4-disubstituted pyrimidines were also prepared. Sequential substitutions to a 4,6-dichloropyrimidine core provided a series of 4,6-disubstituted compounds. 2,4-disubstituted pyrimidines were synthesized via an analogous synthetic route with the pyrimidine C4 affixed as either *p*-trifluoromethoxy aniline or an *m*-aryl benzamide while the pyrimidine C2 was substituted with various groups (Tables S1 and S2 and Scheme S1).

Compounds were first screened against DENV2 NGC at 75 μ M using the viral infectivity assay outlined in Figure 2A. Compounds with appreciable anti-DENV2 activity in this assay were then evaluated at 25 μ M (Table S1). In parallel, the activity of compounds against Abl kinases was determined by six-point titration with the BCR-Abl Ba/F3 cell assay (Table S2). While most of the 4,6-disubstituted analogs lacked activity against DENV2, compounds **3a** and **5a** reduced the single-cycle yield of infectious DENV2 by 10- to 100-fold in comparison to a DMSO control. Importantly, the most potent compound in this series, compound **5a**, is structurally similar to GNF-2 but with considerably lower activity against BCR-Abl.

Most of the 2,4-disubstituted pyrimidine analogs with a trifluoromethoxy aniline at the C4 position are more potent than their 4,6-disubstituted counterparts in the DENV2 infectivity assay, although 2,4-disubstituted pyrimidine analogs with aryl benzamide at the C4 position are less potent. Compounds **8a**, **8b**, and **8c** in this series were the most potent, reducing DENV2 infectivity to undetectable levels (Table S1). A further focused SAR study was performed on analogs containing an *ortho*- or *meta*-trifluoromethoxy substituted aniline at the 2-position of the 2,4-pyrimidine ring (Table 1). IC₉₀ values were defined as the concentration of compound required to reduce single-cycle viral yield by ten-fold in the viral infectivity assay as depicted in Figure 2A. We determined IC₉₀ values for these compounds and selected compounds from earlier rounds of medicinal chemistry against DENV2 NGC

as well as strains representative of the other three DENV serotypes (DENV1 WP74, DENV3 THD1, DENV4 TVP360).

As expected, these newly synthesized compounds were similar to the two leads, **8b** and **8c**, with inhibitory activity against DENV2 NGC comparable to **8b** and **8c** and with greater than 100-fold reduced activity against Bcr-Abl ($IC_{50} > 10 \mu\text{M}$ in the Ba/F3 BCR-Abl cell-based assay). General structure-activity relationship trends are summarized in Figure 2B. As reflected by IC_{90} values, antiviral potencies in the single-digit micromolar range were observed against all four DENV strains tested but with clear variability in the sensitivity of different strains to each compound. The most potent compounds against each strain exhibited IC_{90} values between 1 and 5 μM , representing a ten-fold or greater increase in activity over GNF-2. In general, the compounds in Table 1 have greatest inhibitory activity against DENV2 NGC and DENV1 WP74 (1 μM IC_{90} values $> 20 \mu\text{M}$), and inhibition of these two strains largely tracked together. Antiviral activity is most variable against DENV4 strain TVP360 and least potent against DENV3 strain TDH3. Compound **11h** is an exception to this, exhibiting more potent inhibition of DENV3 TDH3 (IC_{90} 5 μM) and less activity against isolates of DENV1 (IC_{90} $\sim 20 \mu\text{M}$), DENV2 (IC_{90} $\sim 20 \mu\text{M}$), and DENV4 (IC_{90} $\sim 40 \mu\text{M}$). Addition of a trifluoromethoxy group at the *para* position of the benzyl amine in compound **11i** significantly reduces activity against DENV3 THD3 while improving activity against DENV1 WP74 and DENV2 NGC and having a minor effect against DENV4 TVP360. Additional compounds with comparably potent activity against three of four serotypes (IC_{90} $< 10 \mu\text{M}$) but significantly decreased activity against a single serotype (IC_{90} $> 40 \mu\text{M}$) included compounds **8b** (DENV1, -2, -3), **12c** (DENV1, -2, -4), and **12d** (DENV1, -2, -4).

The variable activity against different DENV strains suggested that the antiviral activity is not due to general cytotoxicity, an interpretation we confirmed by measuring cell viability in dose-response assays (Table 1). All CC_{90} values were 5- to >100 -fold higher than IC_{90} values. To show the antiviral potential of the compounds under conditions more relevant to a clinical setting, we also performed experiments demonstrating antiviral activity over multiple replication cycles when cells were infected at low multiplicity of infection (MOI 0.01) and compound treatment delayed until 24 hours post-infection (Figure 2C). Time-of-addition experiments were performed for a subset of compounds to verify that the antiviral activity is, as is the case for GNF-2, due to an effect on events early in the DENV replication cycle (Figure 2D and data not shown). Interestingly antiviral activity appears to be temperature-dependent since we observe no inhibition of DENV2 when the viral inoculum is preincubated with compound at 4 °C (Figure 2D and data not shown). These data demonstrate inhibition of diverse DENV strains by GNF-2-based inhibitors in the viral infectivity assay while also revealing SAR that may be strain-specific (or serotype-specific).

GNF2 derivatives interact with DENV2 virions

Since the target mediating the effect of GNF-2 and related disubstituted pyrimidines on events early in the DENV2 infectious cycle is present in the viral inoculum, we reasoned that the target is likely the virion itself. To test this we first confirmed that a previously reported biotin-conjugated analog of GNF-2, GNF2-biotin (Choi, et al., 2009), inhibits

DENV2 in the viral infectivity assay (IC₉₀ 15 μM, Figure S1) and then tested its interaction with DENV2 NGC virions (Figure 3A). Incubation of GNF2-biotin with purified virions led to capture of DENV2 on streptavidin beads, as evidenced by detection of the DENV envelope protein, E, by Western blot analysis of the affinity-purified eluate (Figure 3B). This interaction is virus-specific and correlated with antiviral activity since we detect no interaction of GNF2-biotin with virions of DENV3, which is inhibited by GNF-2 with an IC₉₀ > 60 μM, or with vesicular stomatitis virus (VSV), an enveloped virus unrelated to DENV (Figure 3B and 3C). The interaction of DENV2 virions with GNF2-biotin also appears to be temperature-dependent, consistent with the idea that conformational dynamics of the virion are required for inhibition (Figure 3C).

To visualize how the interaction of GNF-2 and related compounds with DENV2 virions may affect viral infection, we synthesized a derivative of GNF-2 conjugated to the fluorescent dye Cy5 (GNF2-Cy5) and verified that it retained the anti-DENV2 activity of GNF-2 (IC₉₀ 20 μM, Figure S1). This compound was used in imaging studies in which we monitored the localization of the inhibitor via Cy5 fluorescence and localization of virus by immunofluorescence detection of the DENV E protein during viral entry (Figure 4A). Briefly, purified DENV2 virions were pre-incubated with GNF2-Cy5 for 45 minutes at 37 °C and the mixture was then used to infect Vero cells at an MOI of 10 for 60 minutes at 37 °C, conditions that permit binding and clathrin-dependent uptake of virions. GNF2-Cy5 was incubated with conditioned medium (“No Virus”) or with VSV as negative controls. The cells were washed extensively to remove extracellular GNF2-Cy5 and DENV2 and then fixed, followed by visualization of internalized virus by immunofluorescence staining for the DENV E protein. As shown in Figure 4B, DENV2 is efficiently internalized under these conditions. In the absence of DENV2, essentially no intracellular GNF2-Cy5 signal is observed demonstrating the inability of this compound to penetrate the plasma membrane and the efficient removal of extracellular compound during the wash steps. In contrast, robust, intracellular GNF2-Cy5 signal is observed when the compound is incubated with cells in the presence of DENV2; moreover, the majority of this intracellular Cy5 signal co-localizes with E. Uptake of GNF2-Cy5 into cells appeared to be DENV2-specific since it was not observed with vesicular stomatitis virus (VSV) (Figure 4B), consistent with the affinity capture of DENV2 but not VSV virions by GNF2-biotin (Figure 3B). Together, these data demonstrate that internalization of GNF2-Cy5 is dependent upon the presence of DENV2 and suggest that a specific interaction between the small molecule and the virus occurs extracellularly and is maintained even after the virion has been internalized.

GNF2 derivatives interact with recombinant E in its prefusion state

To identify the molecular target of GNF-2 and the related inhibitors, we reasoned that the most likely candidate is the DENV envelope protein, E, the major protein on the virion surface (Zhang, et al., 2003; Zhang, et al., 2013). Variable activity against strains of the four DENV serotypes also suggested E as the target mediating this antiviral activity since the serotypes are defined by sequence differences of E. E performs essential functions during viral entry, mediating both the initial attachment to the plasma membrane of the host cell as well as catalysis of fusion of the viral and endosomal membranes. This fusion event is coupled to structural reorganization and refolding of E as a post-fusion trimeric species upon

exposure to acidic pH. The time-of-addition experiments are temporally consistent with a mechanism in which E's function in viral entry is inhibited by GNF-2 and related compounds.

To test the hypothesis that GNF-2 and related inhibitors directly target the pre-fusion form of E that exists on mature virions, we examined the interaction of GNF2-biotin with a recombinant, soluble form of the DENV2 E protein (sE) containing the three ectodomains (DI, DII, and DIII) but lacking the stem region and membrane-associated portions of the native protein (Klein, et al., 2013). We developed a bead-based amplified luminescent proximity homogenous assay ("Alpha") screen assay by immobilizing GNF2-biotin and recombinant, prefusion sE on donor and acceptor beads, respectively. The Alphascreen signal detected increases in a concentration-dependent manner with increased loading of the donor beads with GNF2-biotin (Figure 5A). Increasing concentrations of parent compound GNF-2 or compound 3-110-22, a previously published inhibitor of DENV2 infectivity (IC₉₀ 0.77 μM) shown to bind to E (Schmidt, et al., 2012), decrease the Alphascreen signal (Figure 5B); moreover, competition of GNF-2 and 3-110-22 with GNF2-biotin in this assay is correlated with antiviral potency. Biolayer interferometry experiments indicate that GNF2-biotin and prefusion sE interact with low micromolar affinity (Figure S2). We additionally used fluorescence polarization to monitor interaction of a FITC-conjugated derivative of GNF-2 (GNF2-FITC (Deng, et al., 2010); IC₉₀ ~20 μM; Figures 5C and S1) with DENV2 sE in its prefusion and postfusion conformations (Figure 5D). Incubation of GNF2-FITC with increasing concentrations of sE in the prefusion conformation (sE dimer) led to a decrease in fluorescence anisotropy but no change in anisotropy was observed in the presence of increasing concentrations of E in its low-pH-induced, post-fusion trimeric conformation (sE trimer). Thus, GNF2-FITC interacts directly with E in the form that exists on infectious virions.

DISCUSSION

Following our initial report describing the utility of protein kinase inhibitors to probe the DENV replication cycle (Chu and Yang, 2007), we pursued here in detail the mechanism of action of GNF-2, an allosteric inhibitor of Abl kinases. Based on time-of-addition experiments and GNF-2's enhanced anti-DENV2 activity compared to imatinib, we hypothesized that GNF-2 has a dual-action mechanism that includes activity against an extracellular target. We used medicinal chemistry to identify GNF-2 analogs that have lost activity against Abl kinases but have improved activity in the viral infectivity assay. Following the synthesis and testing of various 4,6- and 2,4-disubstituted pyrimidines for activity against DENV2, 2,4-diamino pyrimidines emerged as the most potent inhibitors with IC₉₀ values in the range of 5–20 μM (Table 1). Variability in activity against multiple DENV strains was, at least in part, correlated with DENV serotype, suggesting that GNF-2's extracellular antiviral target might be the DENV E protein—the primary determinant of DENV serotype.

We demonstrated that biotin- and FITC-conjugated derivatives of GNF-2 are able to bind to both DENV2 virions (Figure 3) and to recombinant, soluble DENV2 E protein in the prefusion conformation (Figures 5 and S2). The interaction of recombinant DENV2

SIGNIFICANCE

Dengue virus is a serious human pathogen for which no drug or broadly protective vaccine is currently available. Here we describe the discovery of a series of pyrimidines that can bind to the dengue virus envelope protein, E, and that exhibit anti-viral activity. These findings provide pharmacological validation of the DENV E protein as a new potential anti-viral target and provide lead compounds that can be further optimized. We also demonstrate that GNF-2 has a dual mechanism of anti-viral action with antiviral activities mediated by two independent targets, the viral E protein on the virion surface as well as intracellular Abl kinases. Given the success of polypharmacological kinase inhibitors in suppressing drug resistance in oncology, GNF-2 or related dual-acting compounds provide a means to address whether polypharmacology may be useful in suppressing antiviral resistance.

EXPERIMENTAL PROCEDURES

METHODS AND MATERIALS

Cells and virus—All work with infectious dengue virus was performed in a biosafety level 2 (BSL2) laboratory using additional safety practices as approved by the Harvard Committee on Microbiological Safety. Human hepatoma Huh-7 cell line and Vero African green monkey kidney cells were cultured in DMEM medium with 10% FBS at 37°C with 5% CO₂. C6/36 cells, a continuous mosquito cell line derived from *Aedes albopictus* (Diptera: Culicidae) embryonic tissue was grown in L-15 medium containing 10 % FBS at 28 °C. Both Huh-7 and Vero cells were purchased from ATCC. C6/36 cells and the dengue serotype 2 strain New Guinea C (DENV2 NGC) were kind gifts from Lee Gerhke (Massachusetts Institute of Technology). NIH3T3 cells and Abl-deficient 3T3 cells (c-Abl^{-/-}) were kindly provided by Anthony Kolesky (Yale University) and were maintained in DMEM medium with 10% FBS at 37°C with 5% CO₂. Dengue strains DENV1 WP74, DENV3 THD3, and DENV4 TVP360 were generous gifts from Aravinda De Silva (University of North Carolina – Chapel Hill).

All virus stocks were grown in C6/36 cells in L-15 medium supplemented with 2% FBS. Cells were infected for 1 hour at 25 °C, then overlaid with medium and incubated at 25 °C until syncytium formation was observed. The supernatant was clarified by centrifugation at 4 °C and stored at –80 °C.

Virus used in affinity chromatography and microscopy experiments was further purified by polyethylene glycol precipitation followed by centrifugation on a potassium tartrate step gradient. Additional details are provided as Supplemental Experimental Procedures..

Antibodies—Monoclonal antibody 4G2 against the DENV E protein was produced from culture supernatants of hybridoma D1-4G2-4-15, ATCC® HB-112™. Mouse hybridomas producing monoclonal antibody 6F3.1 against DENV2 core protein were generously provided by John Aaskov (Queensland University of Technology) (Bulich and Aaskov, 1992).

Compound synthesis and characterization—Detailed descriptions of synthetic methods and compound characterization are provided as Supplemental Experimental Procedures.

Recombinant proteins and antibodies—Recombinant, soluble DENV2 E protein (sE) in the prefusion, dimeric conformation was expressed in insect cells using a recombinant baculovirus system and was purified as previously described (Klein, et al., 2013). The prefusion form of the protein was converted to soluble post-fusion trimer as described (Modis, et al., 2004).

Virus infections—Unless otherwise indicated, cells were infected by incubation of a confluent monolayer with viral inoculum at the indicated multiplicity of infection (MOI) for one hour at 37 °C. The inoculum was then removed, and the cells were washed twice with phosphate-buffered saline (PBS). The appropriate medium was overlaid on the cells.

Quantification of viral titer by plaque- and focus-formation assay—DENV2 titers were quantified by plaque formation assay on BHK21 cells. DENV1 and DENV4 titers were quantified by focus formation assay on BHK21 cells. DENV3 titers were quantified by focus formation assay on Vero cells. 10⁵ cells/well (BHK-21 cells for DENV1, 2, and 4; Vero for DENV3) were seeded in a 24-well plate and left overnight at 37°C to form a confluent monolayer. Ten-fold serial dilutions of the supernatant were made in Earle's balanced salt solution (EBSS) and 100 µL of each dilution was used to infect one well for one hour at 37°C, after which cells were washed once with 1X PBS. Overlay medium (1.05% CMC with MEM α , 2% FBS, penicillin-streptomycin antibiotics for BHK-21; 1.05% CMC with DMEM, 2% FBS, penicillin-streptomycin for Vero) and plates were incubated for 5 (BHK-21) or 6 days (Vero). Assays were washed twice with 1X PBS to remove overlay medium and cells were fixed. For DENV2, plaque-forming units (pfu/mL) were measured by staining the cells with crystal violet and counting the number of plaques. For DENV1, DENV3, and DENV4, cells were fixed with 3.7% formaldehyde for 15 minutes at room temperature, followed by a 15 minute incubation at RT with 20 mM NH₄Cl. Cold 60/40 (vol/vol) methanol/acetone was added and plates were kept at -20°C until staining (30 minutes – overnight). To visualize foci, monolayers were blocked with 1% FBS and 0.1% Tween-20 in 1X PBS for 10 minutes at room temperature and then incubated with 1:1000 dilution of mouse monoclonal antibody 4G2 for 30 minutes at 37°C. Plates were incubated with horseradish peroxidase goat-anti-mouse antibody (1:500) for 30 minutes at 37°C and foci were visualized using the Vector VIP substrate kit (Vector Labs, Cat#SK4600).

Order of addition and multicycle infection experiments—Experiments were carried out in BHK-21 cells using DENV2 NGC in the presence of 15 µM of GNF-2 or imatinib at times noted in schematic. All virus was diluted in EBSS to achieve a multiplicity of infection (MOI) of 1. Cells or virus were pre-incubated in 100 µL medium containing compounds for one hour at 37°C (“PRE cells” and “PRE virus”). For co-infection, 15 µM of compound was added to the virus inoculum directly before addition to cells (“CO”). After an initial one hour infection, cells were washed twice with 1X PBS to remove unbound compound and virus and 1 mL cell medium (MEM-alpha with 2% FBS). At 1 or 5 hours

post-infection, medium was replaced with compound-containing medium. 24 hours after initial infection, culture supernatant was collected, and the yield of infectious particles was determined by plaque formation assay.

To examine antiviral activity under conditions of low multiplicity of infection and multiple infectious cycles, BHK-21 cells were infected with DENV2 NGC at an MOI of 0.01 as described above. At 24 hours post-infection, inhibitors GNF-2 (15 μ M) or **8b** (5 μ M) were added. Viral titers were quantified by plaque formation assay at 24 hours post-infection (prior to inhibitor addition) and at 48 and 72 hours post-infection.

Viral infectivity assays for IC₉₀ determination—Virus inocula were pre-incubated with compounds at the indicated final concentrations for 45 minutes at 37 °C. The mixture was then overlaid on cells for one-hour at 37 °C to allow infection, after which the inoculum was removed and the cells were washed twice with PBS to remove unbound virus and compound. Cells were overlaid with medium and incubated at 37 °C for 24 hours, corresponding to a single-cycle of infection. Culture supernatants were harvested at this time, and the yield of infectious particles produced was quantified by viral plaque formation assay. For IC₉₀ value determinations, a 6-point titration curve with each compound was performed. The IC₉₀ value corresponds to the empirically determined, minimal concentration of compound that reduces the single-cycle viral yield by ten-fold under these experimental conditions.

RNAi and MEF experiments—A pool of four siRNAs targeting c-Abl kinase (NCBI accession no. NM_005157), and a non-targeting siRNA pool were purchased from Dharmacon, Chicago, IL). The pool of siRNAs (final concentrations of 100 nM and 50 nM) was reverse-transfected into Huh-7 cells (cell density of 1×10^3 cells) using HiPerfect (Qiagen, Valencia, CA) according to the manufacturer's instructions. The effects of siRNA knockdown on intracellular levels of clathrin and c-Abl kinase were verified by Western blotting and immunofluorescence assays. 48 hours after the reverse transfection, cells were infected with DENV2 NGC at an MOI of 1 as described above and then incubated at 37 °C. Murine embryo fibroblasts deficient in c-Abl (Ab^{1-/-}) and wildtype 3T3 cells were infected at MOIs of 1 and 10. 72 hours post-infection, culture supernatants were harvested, and viral titers were measured by plaque formation assay.

Affinity capture of dengue virions with GNF2-biotin—DENV particles were purified by density centrifugation as described above. Total protein in the purified virus prep was determined by Bradford assay. 300–400 ng purified virions were incubated with varying concentrations of GNF2- biotin for 45 minutes at 37°C in 200 μ L HNE buffer (5 mM HEPES, 150 mM NaCl, 0.1mM EDTA; pH 7.4). Streptavidin resin (GE Biosciences, Cat. #17-5113-01) was prepared by two rinses with HNE buffer, followed by blocking with HNE buffer supplemented with 5% FBS for one hour at 4°C. The resin was then resuspended in HNE buffer. 20 μ L resin was added to the GNF2-biotin and virus solution and incubated for 20 minutes at 4°C. Each sample was washed ten times with 1 mL HNE buffer before being resuspended in 20 μ L Laemmli sample buffer without beta-mercaptoethanol (BioRad, Cat. #161-0737). Samples were boiled (>95°C) for 20 minutes, spun down, and then fractionated on a 10% SDS-PAGE gel. Proteins were transferred to PVDF membrane by semi-dry

transfer (10V, 1.5 hrs) and membranes were then probed by Western blotting for E protein using monoclonal antibody 4G2. Immunoblots were visualized by chemiluminescence (Pierce ECL reagent cat#32106) following the manufacturer's instructions.

Fluorescence microscopy of DENV and GNF2-Cy5—Vero cells (3×10^4) were plated on coverslips for infection with purified DENV2 (0.5 μg) that had been incubated with 25 μM GNF2-Cy5 at 37°C for 1.5 hours. Cells were infected for 30 minutes at 37°C, then washed three times with 1X PBS to remove unbound virus or compound and fixed with methanol. Coverslips were then stained for the DENV E protein (US Biological, Cat. #D2810-05, 1:200) and visualized using FITC-conjugated goat anti-mouse secondary (Jackson Laboratories Cat. #115-095-146, 1:400). Images were acquired at 600X magnification. Z-stacks were recorded to confirm co-localization of the signals for GNF2-Cy5 and E. Images shown are representative of a broad field of view.

Alphascreen assay—Assays were performed with Ni-chelate acceptor beads and streptavidin donor beads (Perkin-Elmer) with final concentration each of 25 $\mu\text{g}/\text{mL}$ donor and acceptor beads in $1 \times$ Kinetic buffer (Pall ForteBio). Briefly, Ni-chelate acceptor beads were incubated with 3 to 200 μM GNF2-biotin and 50 nM DENV2 sE protein in the dark at room temperature for 2 hours. Streptavidin beads were then added, and the mixture was incubated an additional 2 hours in the dark. Assay plates were read using laser excitation at 680 nm with emission detected at 520 to 620 nm on an EnVision plate reader.

Cross-titration experiments were performed to determine protein and GNF2-biotin concentrations that lead to saturation of the Alphascreen signal, and competition experiments were performed at concentrations of the two binding partners that produced 80% of the saturated signal. The Alphascreen assay was then performed as above but with the inclusion of inhibitors GNF-2, **11g**, and 3-110-22 at final concentrations of 20 nM to 10 μM in the initial incubation of Ni-chelate acceptor beads with GNF2-biotin and DENV2 sE protein.

Bio-layer interferometry experiment—Streptavidin (SA) biosensor tips (Pall ForteBio) were hydrated in running buffer (50 mM TAN, pH 8.0, with 150 mM NaCl and 0.1% Tween 20) for at least 10 min at room temperature and then blocked in blocking buffer (50 mM triethanolamine, pH 8.0, with 150 mM NaCl and 5 ~ 10% FBS) for 3 to 10 min at room temperature prior to running Blitz experiments. SA tips were saturated with 25 μM GNF2-biotin or DMSO (as control) for 200s-300s. Baseline was then collected in 60s in running buffer. sE (wt) at different concentrations (from 1 to 8 μM) was bound to the GNF2-biotin for 120s and allowed to dissociate into running buffer for 120s. The data were analyzed by using the ForteBio Pro software for both global and local (1:1) fitting.

Fluorescence polarization assay—Stock concentrations of GNF2-FITC were made in DMSO and dissolved in assay buffer immediately before use. GNF2-FITC was incubated with DENV2 sE prefusion dimer at final concentrations of 0.1 to 25.6 μM or with DENV2 sE postfusion trimer at final concentrations of 75 nM to 4.8 μM in TAN buffer (20mM triethanolamine, 100mM NaCl, pH 8.0). Each well contained a final volume of 20 μL . Reactions were incubated at 37 degrees C for 2 hours and then read using a Perkin Elmer

EnVision instrument with excitation wavelength of 485nm and emission wavelength of 535 nm.

Supplementary Material

Refer to Web version on PubMed Central for supplementary material.

Acknowledgments

We gratefully acknowledge Anthony Koleske for the gifts of the Abl-deficient and wildtype 3T3 cell lines; Jae Won Chang for synthesis of GNF2-Cy5; John Aaskov for hybridomas expressing 6F3.1; and Lee Gehrke, Aravinda De Silva, Sean Whelan, and Marylyne Yates for viruses. Stephen C. Harrison and Daryl Klein provided helpful discussions and assistance in expression of recombinant sE. We thank the Center for Macromolecular Interactions in the Department of Biological Chemistry and Molecular Pharmacology and the Harvard ICCB-Longwood Screening Facility for instrument usage and support. This work was supported by a Harvard Medical School Faculty Development Grant (NSG, PLY), an Armenise-Harvard Junior Faculty Grant (PLY); and NIH Grants R01 CA130876 (NSG), R01 AI076442 (PLY), R01 AI095499 (PLY, NSG), R56 AI095499 (PLY), U19 AI109740 (S. Whelan), U54 AI057159 (D. Kasper), and a Catalyst grant from the Harvard Clinical and Translational Science Center (NIH UL1TR001102, L. Nadler).

References

- Adrian FJ, Ding Q, Sim T, Velentza A, Sloan C, Liu Y, Zhang G, Hur W, Ding S, Manley P, et al. Allosteric inhibitors of Bcr-abl-dependent cell proliferation. *Nat Chem Biol.* 2006; 2:95–102. [PubMed: 16415863]
- Austin SK, Dowd KA, Shrestha B, Nelson CA, Edeling MA, Johnson S, Pierson TC, Diamond MS, Fremont DH. Structural basis of differential neutralization of DENV-1 genotypes by an antibody that recognizes a cryptic epitope. *PLoS Pathog.* 2012; 8:e1002930. [PubMed: 23055922]
- Bhatt S, Gething PW, Brady OJ, Messina JP, Farlow AW, Moyes CL, Drake JM, Brownstein JS, Hoen AG, Sankoh O, et al. The global distribution and burden of dengue. *Nature.* 2013; 496:504–507. [PubMed: 23563266]
- Bulich R, Aaskov JG. Nuclear localization of dengue 2 virus core protein detected with monoclonal antibodies. *J Gen Virol.* 1992; 73(Pt 11):2999–3003. [PubMed: 1279106]
- Carocci M, Hinshaw SM, Rodgers MA, Villareal VA, Burri DJ, Pilankatta R, Maharaj NP, Gack MU, Stavale EJ, Warfield KL, et al. The bioactive lipid 4-hydroxyphenyl retinamide inhibits flavivirus replication. *Antimicrob Agents Chemother.* 2015; 59:85–95. [PubMed: 25313218]
- Choi Y, Seeliger MA, Panjarian SB, Kim H, Deng X, Sim T, Couch B, Koleske AJ, Smithgall TE, Gray NS. N-myristoylated c-Abl tyrosine kinase localizes to the endoplasmic reticulum upon binding to an allosteric inhibitor. *J Biol Chem.* 2009; 284:29005–29014. [PubMed: 19679652]
- Chu JJ, Yang PL. c-Src protein kinase inhibitors block assembly and maturation of dengue virus. *Proc Natl Acad Sci U S A.* 2007; 104:3520–3525. [PubMed: 17360676]
- de Wispelaere M, LaCroix AJ, Yang PL. The small molecules AZD0530 and dasatinib inhibit dengue virus RNA replication via Fyn kinase. *J Virol.* 2013; 87:7367–7381. [PubMed: 23616652]
- Deng X, Okram B, Ding Q, Zhang J, Choi Y, Adrian FJ, Wojciechowski A, Zhang G, Che J, Bursulaya B, et al. Expanding the diversity of allosteric bcr-abl inhibitors. *J Med Chem.* 2010; 53:6934–6946. [PubMed: 20828158]
- Dowd KA, Jost CA, Durbin AP, Whitehead SS, Pierson TC. A dynamic landscape for antibody binding modulates antibody-mediated neutralization of West Nile virus. *PLoS Pathog.* 2011; 7:e1002111. [PubMed: 21738473]
- Kampmann T, Yennamalli R, Campbell P, Stoermer MJ, Fairlie DP, Kobe B, Young PR. In silico screening of small molecule libraries using the dengue virus envelope E protein has identified compounds with antiviral activity against multiple flaviviruses. *Antiviral Res.* 2009; 84:234–241. [PubMed: 19781577]
- Klein DE, Choi JL, Harrison SC. Structure of a dengue virus envelope protein late-stage fusion intermediate. *J Virol.* 2013; 87:2287–2293. [PubMed: 23236058]

- Koleske AJ, Gifford AM, Scott ML, Nee M, Bronson RT, Miczek KA, Baltimore D. Essential roles for the Abl and Arg tyrosine kinases in neurulation. *Neuron*. 1998; 21:1259–1272. [PubMed: 9883720]
- Lok SM, Kostyuchenko V, Nybakken GE, Holdaway HA, Battisti AJ, Sukupolvi-Petty S, Sedlak D, Fremont DH, Chipman PR, Roehrig JT, et al. Binding of a neutralizing antibody to dengue virus alters the arrangement of surface glycoproteins. *Nat Struct Mol Biol*. 2008; 15:312–317. [PubMed: 18264114]
- Modis Y, Ogata S, Clements D, Harrison SC. A ligand-binding pocket in the dengue virus envelope glycoprotein. *Proc Natl Acad Sci U S A*. 2003; 100:6986–6991. [PubMed: 12759475]
- Modis Y, Ogata S, Clements D, Harrison SC. Structure of the dengue virus envelope protein after membrane fusion. *Nature*. 2004; 427:313–319. [PubMed: 14737159]
- Poh MK, Yip A, Zhang S, Priestle JP, Ma NL, Smit JM, Wilschut J, Shi PY, Wenk MR, Schul W. A small molecule fusion inhibitor of dengue virus. *Antiviral Res*. 2009; 84:260–266. [PubMed: 19800368]
- Schmidt AG, Lee K, Yang PL, Harrison SC. Small-molecule inhibitors of dengue-virus entry. *PLoS Pathog*. 2012; 8:e1002627. [PubMed: 22496653]
- Wang QY, Patel SJ, Vangrevelinghe E, Xu HY, Rao R, Jaber D, Schul W, Gu F, Heudi O, Ma NL, et al. A small-molecule dengue virus entry inhibitor. *Antimicrob Agents Chemother*. 2009; 53:1823–1831. [PubMed: 19223625]
- Yennamalli R, Subbarao N, Kampmann T, McGeary RP, Young PR, Kobe B. Identification of novel target sites and an inhibitor of the dengue virus E protein. *J Comput Aided Mol Des*. 2009; 23:333–341. [PubMed: 19241120]
- Zhang W, Chipman PR, Corver J, Johnson PR, Zhang Y, Mukhopadhyay S, Baker TS, Strauss JH, Rossmann MG, Kuhn RJ. Visualization of membrane protein domains by cryo-electron microscopy of dengue virus. *Nat Struct Biol*. 2003; 10:907–912. [PubMed: 14528291]
- Zhang X, Ge P, Yu X, Brannan JM, Bi G, Zhang Q, Schein S, Zhou ZH. Cryo-EM structure of the mature dengue virus at 3.5-Å resolution. *Nat Struct Mol Biol*. 2013; 20:105–110. [PubMed: 23241927]
- Zhou Z, Khaliq M, Suk JE, Patkar C, Li L, Kuhn RJ, Post CB. Antiviral compounds discovered by virtual screening of small-molecule libraries against dengue virus E protein. *ACS Chem Biol*. 2008; 3:765–775. [PubMed: 19053243]

Highlights

GNF-2 is a polypharmacological inhibitor of dengue virus

GNF-2's inhibition of Abl kinases affects dengue virus at a post-entry step

GNF-2 inhibits dengue virus entry through direct interaction with the viral E protein

Author Manuscript

Author Manuscript

Author Manuscript

Author Manuscript

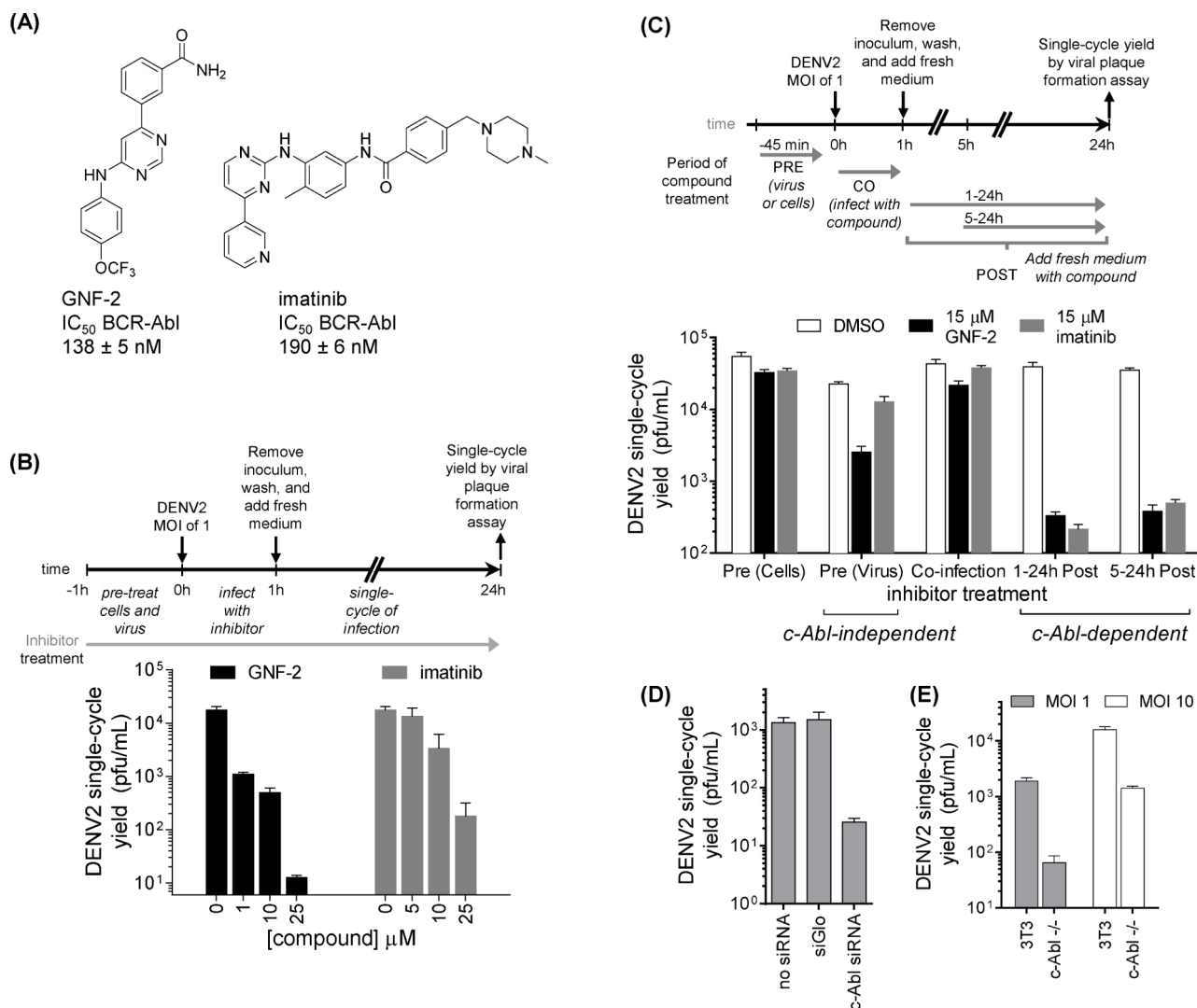


Figure 1. GNF-2's inhibition of DENV2 is mediated by cellular Abl kinases and an additional target not shared with imatinib

(A) Structures of Abl kinase inhibitors GNF-2 and imatinib. (B–E) Infections were performed by incubating cells with DENV2 NGC inoculum for one hour at 37 degrees, after which the cells were washed to remove non-adsorbed virus. Unless otherwise indicated, all infections were performed at a multiplicity of infection (MOI) of 1. To quantify antiviral effects, culture supernatants were harvested at 24 hours post-infection (hpi), corresponding to a single-round of infection, and the yield of infectious viral particles was quantified by viral plaque formation assay. (B) GNF-2 exhibits greater antiviral potency than imatinib in dose-response experiments quantifying the effect of inhibitor when present during the entirety of a single round of DENV2 NGC infection. (C) Time-of-addition experiments were performed by infecting BHK21 cells at MOI of 1 and varying the time of inhibitor treatment. For “PRE” conditions, either cells or viral inoculum were preincubated with imatinib or GNF-2. For “CO” conditions, inhibitors were present during the one hour incubation of viral inoculum with cells. For “POST” conditions, inhibitors were added following the initial one-hour infection and washes. Final inhibitor concentration was 15 μ M for all conditions. Both

GNF-2 and imatinib inhibit DENV2 when added at 0-5 hours post-infection, but only GNF-2 exhibits antiviral activity when preincubated with the DENV2 inoculum prior to infection. **(D)** Cells were reverse-transfected with siRNA Smartpool™ targeting c-Abl or with siGlo control. 48 hours later, cells were infected; viral yields were determined 72 hpi. **(E)** Wildtype 3T3 cells or murine embryo fibroblast (MEF) cells genetically deficient for *c-Abl* were infected with DENV2 NGC at MOI of 1 or 10; viral yields were measured at 72 hpi. The absence of c-Abl due to RNAi or genetic knockout is associated with reduced DENV2 replication. Each experiment was performed $n = 2$, and viral plaque formation assays were performed in triplicate. Representative data are shown for the mean \pm stdev of the viral plaque formation assays for a representative experiment.

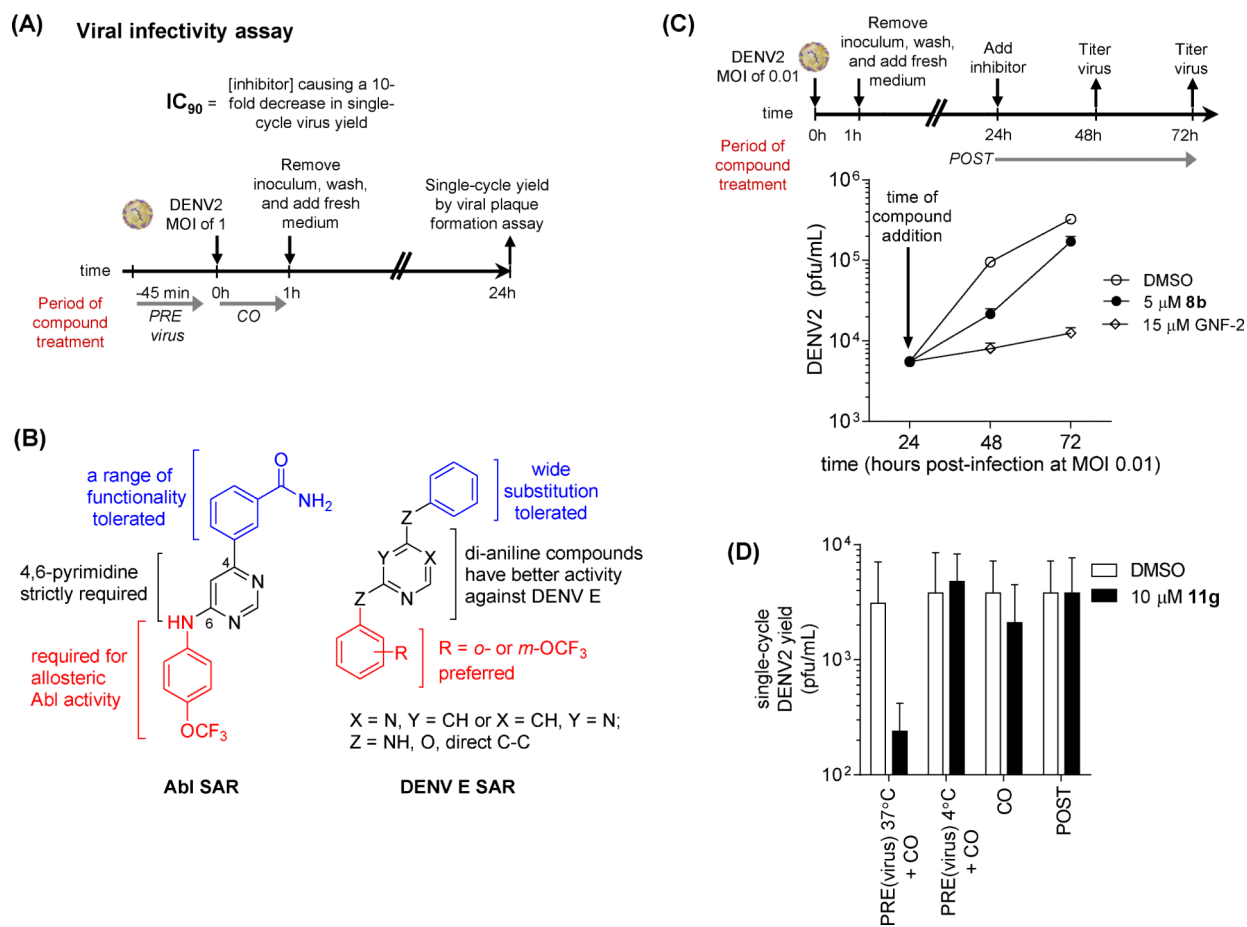


Figure 2. GNF-2 analogs that lack activity against Abl kinases inhibit DENV via (A) Schematic of viral infectivity assay measuring the antiviral activity exerted by compounds when preincubated with viral inoculum at 37 degrees C, 45 minutes and when present during the one hour incubation of cells with the viral inoculum but absent for the remainder of the experiment. Single-cycle viral yield was quantified at 24 hpi as a readout for inhibition of viral infectivity during the initial infection. (B) Summary of structure-activity relationships (SAR) distinguishing inhibition of Abl kinases and antiviral activity measured in the viral infectivity assay. While trends for anti-DENV activity are derived from data against all four DENV serotypes as listed in Tables 1 and S1, the observed trends are most robust for DENV2 and DENV1. (C) Both GNF-2 and **8b inhibit DENV2 in a low multiplicity of infection (MOI 0.01), multiple replication cycle experiment when inhibitor treatment is delayed until 24 hpi. Culture supernatants were harvested at 24, 48, and 72 hpi to allow quantification of viral titers and demonstration of antiviral activity. (D) Inhibition of DENV2 in the viral infectivity assay (Figure 2A) is lost if incubation of inhibitor with viral inoculum is performed at 4 degrees C. Data are shown for compound **11g**; analogous experiments were performed for other analogs in Table 1. Each experiment was performed $n = 2$, and viral plaque formation assays were performed in triplicate (A, D) or duplicate (C). Representative data are shown for the mean \pm stdev of the viral plaque formation assays for a representative experiment.**

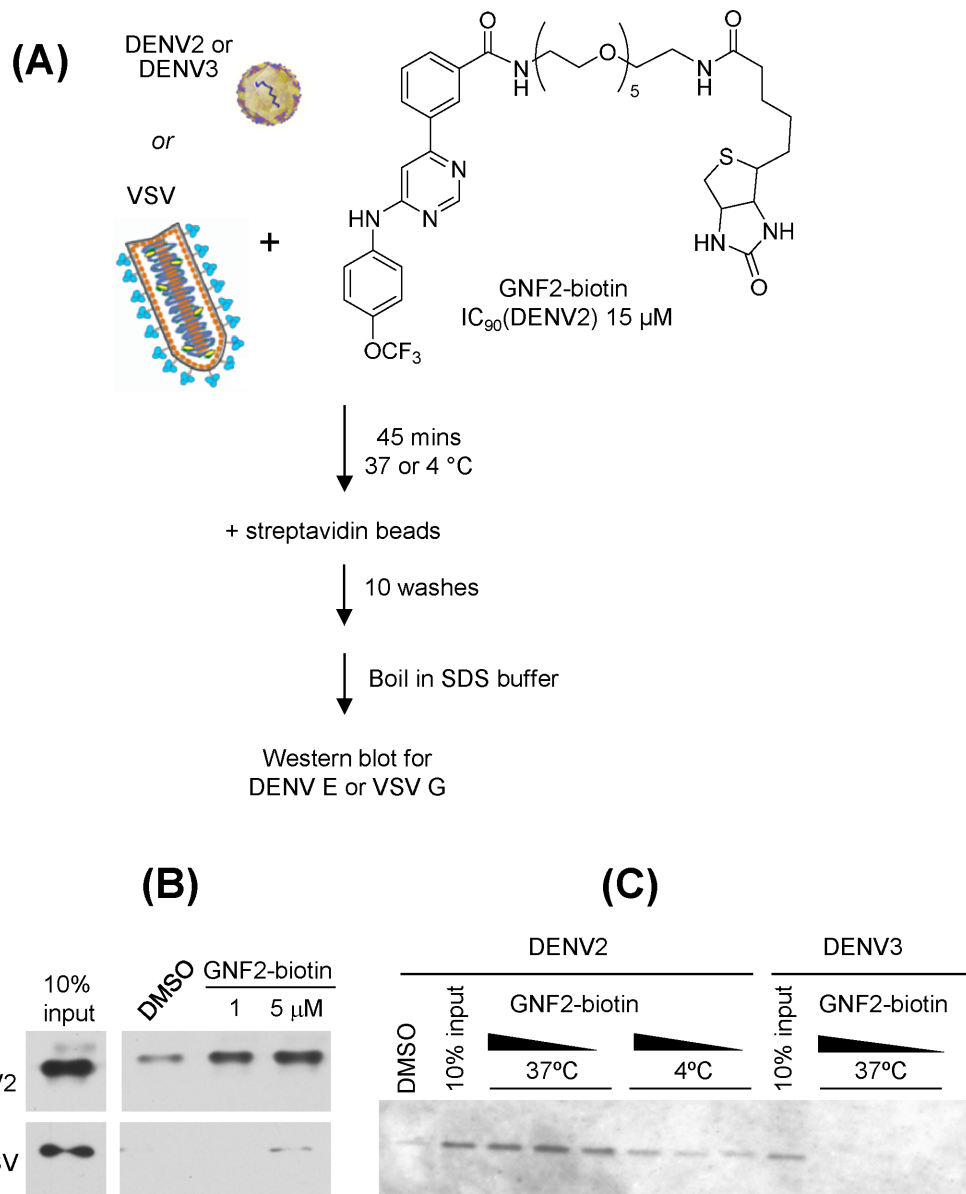


Figure 3. GNF2-biotin interacts specifically with dengue virions

(A) Structure of GNF2- biotin and schematic of experiment to detect its interaction with dengue virions. (B) DENV2 NGC virions but not vesicular stomatitis virions are captured on streptavidin-derivatized beads in the presence of GNF2-biotin. (C) Affinity capture of dengue virions is more efficient at 37 degrees C than at 4 degrees C and is correlated with the sensitivity of the virus to GNF-2, as evidenced by little or no affinity capture of DENV3 TDH3 virions. Representative data for two or more independent experiments are shown.

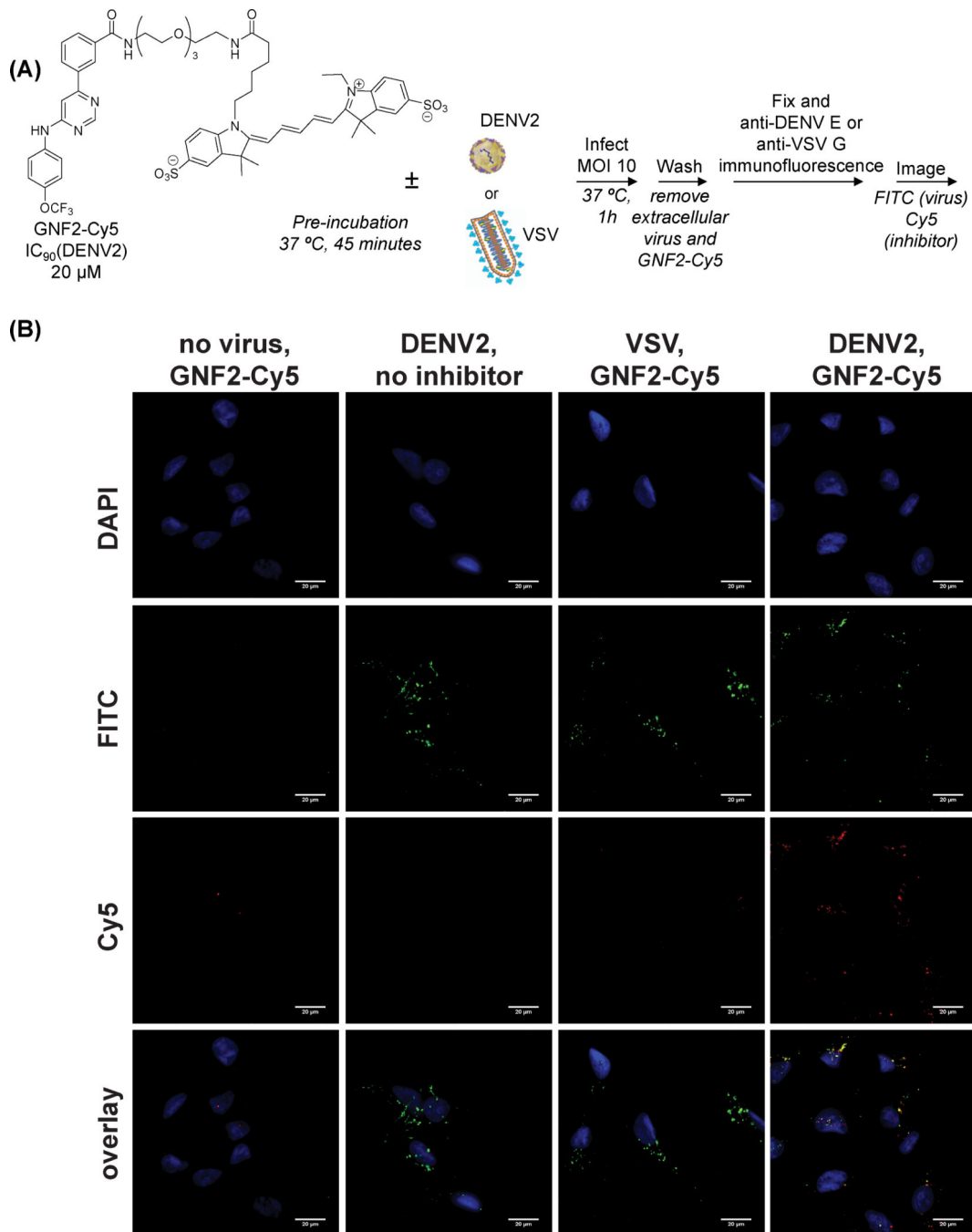


Figure 4. Non-cell permeant GNF2-Cy5 enters cells in the presence of DENV2 and co-localizes with the viral E protein

(A) Structure of GNF2-Cy5 and schematic of experiment to monitor uptake of GNF2-Cy5 into uninfected cells, cells infected with VSV, or cells infected with DENV2 NGC. **(B)** Intracellular GNF2-Cy5 is not detected in uninfected cells or cells infected with VSV but enters cells in the presence of DENV2. Signal for Cy5 colocalizes with E to a significant extent. Scale bars are equal to 20 microns. Representative data for two or more independent experiments are shown.

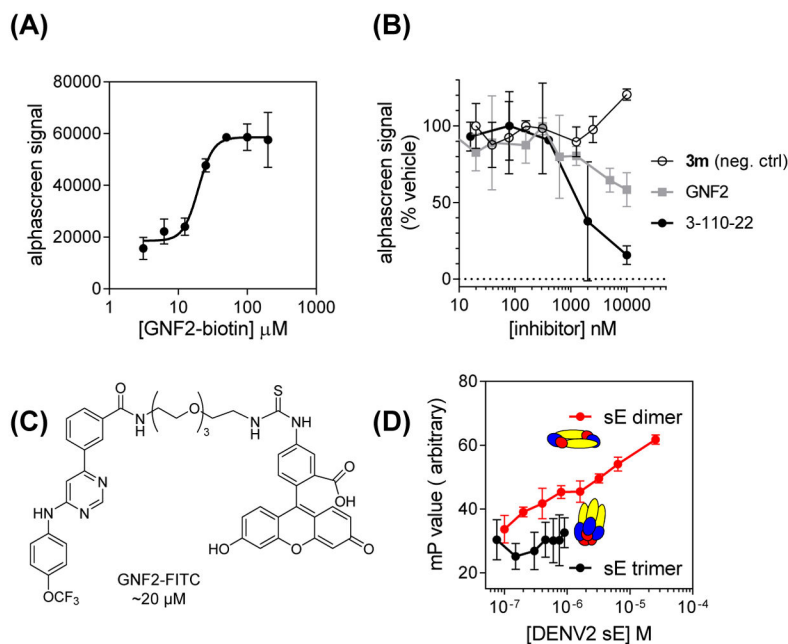
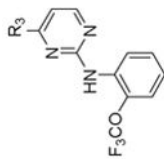
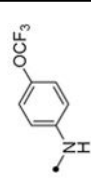
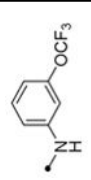
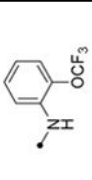
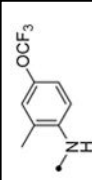
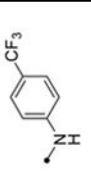
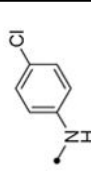
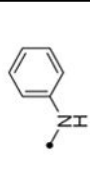


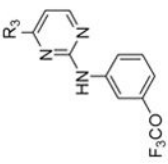
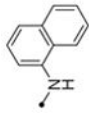
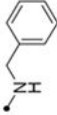
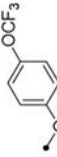
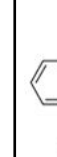
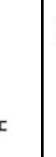
Figure 5. GNF2-FITC and GNF2-biotin bind to prefusion DENV2 E

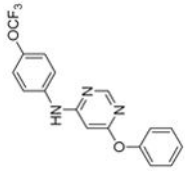
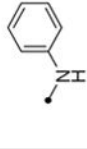
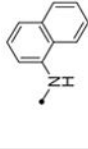
(A) Interaction of GNF2-biotin with a recombinant, soluble form of the DENV2 E protein in its prefusion conformation occurs in a concentration-dependent manner detectable in a bead-based proximity assay (AlphaScreen). (B) Concentration-dependent disruption of this interaction by representative small molecule inhibitors of DENV2 infectivity is correlated with antiviral potency. Compound **3m** is a negative control compound that exhibits no activity in the DENV2 infectivity assay (Table S1). IC_{90} values in the infectivity assay are GNF-2, 18 μM and 3-110-22, 0.77 μM (Schmidt, et al., 2012). (C) Structure of GNF2-FITC. (D) Interaction of GNF2-FITC with prefusion sE is detectable by increasing anisotropy in a fluorescence polarization assay. No interaction of GNF2-FITC with a soluble form of the DENV2 E protein in the post-fusion, trimeric conformation was detected. Representative data for two or more independent experiments are shown. Data represent the mean \pm standard deviation for a representative experiment performed $n = 2$.

Table 1

Anti- DENV and BCR-Abl activity of a focused library of 2,4-disubstituted pyrimidine analogs and compound 3a.

| Core structure | Compound | R ₃ | IC ₉₀ (μM) | | | | BHK21-DENV2 CC ₉₀ (μM) | Bcr-Abl Ba/F3 IC ₅₀ (μM) |
|---|----------|---|-----------------------|-------|-------|-------|-----------------------------------|-------------------------------------|
| | | | DENV1 | DENV2 | DENV3 | DENV4 | | |
|  | 8b |  | 4 | 5 | 10 | 40 | 60 | >10 |
| | 11a |  | 10 | 17.5 | >40 | 10 | 100 | >10 |
| | 11b |  | 20 | 25 | 40 | >40 | 40 | >10 |
| | 11c |  | 10 | 25 | >40 | 5 | 80 | >10 |
| | 11d |  | 4 | 20 | 30 | >40 | 50 | >10 |
| | 11e |  | 10 | 10 | >40 | 20 | 100 | >10 |
| | 11f |  | 20 | 25 | >40 | 10 | 80 | >10 |

| Core structure | Compound | R ₃ | IC ₉₀ (μM) | | | | BHK21-DENV2 CC ₉₀ (μM) | Bcr-Abl Ba/F3 IC ₅₀ (μM) |
|--|----------|---|-----------------------|-------|-------|-------|-----------------------------------|-------------------------------------|
| | | | DENV1 | DENV2 | DENV3 | DENV4 | | |
|  | 11g |  | 10 | 25 | >40 | >40 | 100 | >10 |
| | 11h |  | 20 | 25 | 5 | 40 | 50 | >10 |
| | 11i |  | 5 | 10 | >40 | 40 | 100 | >10 |
| | 11j |  | 40 | 15 | >40 | 40 | >100 | >10 |
| | 8c |  | 1 | 5 | 40 | 17.5 | 100 | >10 |
| | 12a |  | 1 | 20 | >40 | 10 | 90 | >10 |
| | 12b |  | 1 | 25 | >40 | 15 | 90 | >10 |
| | 12c |  | 3 | 5 | >40 | 10 | 90 | >10 |
| | 12d |  | 3 | 7.5 | 40 | 7.5 | 75 | >10 |

| Core structure | Compound | R ₃ | IC ₉₀ (μM) | | | | BHK21-DENV2 CC ₉₀ (μM) | Bcr-Abl Ba/F3 IC ₅₀ (μM) |
|---|------------|---|-----------------------|-------|-------|-------|-----------------------------------|-------------------------------------|
| | | | DENV1 | DENV2 | DENV3 | DENV4 | | |
|  | 12e |  | 4 | 25 | >40 | 15 | >10 | |
| | 12f |  | 7 | 17.5 | >40 | 35 | >10 | |
| | 3a | | 20 | 7.5 | >40 | 15 | >10 | |

Columns are: 1. core chemical structure; 2. compound code; 3. chemical structure of R₃ group; 4. IC₉₀ values against DENV1-4 viruses in the infectivity assay outlined in Figure 2; 5. CC₉₀ in micromolar for viability of BHK21 cells; 6. IC₅₀ in micromolar for viability of BCR-Abl-dependent murine Ba/F3 cells.